Circular RNA circRGNEF promotes bladder cancer progression via miR-548/KIF2C axis regulation

Chen Yang[1,2,3,*], Qiong Li[4,*], Xinan Chen[1,2,*], Zheyu Zhang[1,2], Zezhong Mou[1,2], Fangdie Ye[1,2], Shengming Jin[5], Xiang Jun[6], Feng Tang[4], Haowen Jiang[1,2,3]

[1]Department of Urology, Huashan Hospital, Fudan University, Shanghai 200040, China
[2]Fudan Institute of Urology, Huashan Hospital, Fudan University, Shanghai 200040, China
[3]National Clinical Research Center for Aging and Medicine, Fudan University, Shanghai 200032, China
[4]Department of Pathology, Huashan Hospital, Fudan University, Shanghai 200040, China
[5]Shanghai Cancer Center, Fudan University, Shanghai 200040, China
[6]Department of Urinary Surgery, Tongji Hospital, Tongji University School of Medicine, Shanghai 200065, China
*Equal contribution

Correspondence to: Xiang Jun, Feng Tang, Haowen Jiang; **email:** wallyxiang@126.com, tangfeng1966@sina.com, urology_hs@163.com

ABSTRACT

Circular RNAs (circRNAs) play an important role in bladder cancer (BC). Though circRNA involvement in BC has been reported, the underlying regulatory mechanisms are unknown. In this study, we performed EdU, CCK8, colony formation and Transwell assays to establish the role of circRGNEF in BC cell migration, proliferation, and invasion. We used bioinformatics and luciferase reporter experiments to investigate the regulatory mechanism. Nude mice xenografts and live imaging were used to explore the role of circRGNEF in tumor metastasis and growth. Expression profile analysis of human circRNAs in BC revealed that circRGNEF was upregulated significantly. High circRGNEF expression was correlated with aggressive BC phenotypes. The downregulation of circRGNEF suppressed BC cell metastasis and proliferation by targeting the miR-548/KIF2C axis *in vitro* and *in vivo*; these results were verified with luciferase reporter assays. Our results show that miR-548 downregulation or KIF2C overexpression restored BC cell proliferation, migration, and invasion following silencing of circRGNEF. KIF2C overexpression reversed miR-548-induced cell invasion and migration as well as growth inhibition *in vitro*. In summary, the data illustrate that circRGNEF suppresses BC progression by functioning as a miR-548 sponge to enhance KIF2C expression. Therefore, circRGNEF might be a candidate BC treatment target.

INTRODUCTION

Bladder cancer (BC) is a type of cancer that occurs primarily in males; it is the primary cause of cancer-related mortalities in men, with 430,000 new cases every year [1–3]. BC is a complex cancer associated with high rates of mortality with no adequate treatment options [4]. To date, there are no perfect treatments for invasive, high grade BC. Chemotherapy and radical cystectomy are alternatives for the treatment of BC.

However, these treatments significantly reduce patient survival and quality of life [5, 6]. Thus, the mechanisms of BC should be investigated to effectively prevent progression.

Circular RNAs (circRNAs) were discovered first in 1976 [7]. Since then, various circRNAs have been identified [8]. circRNAs constitute a conserved endogenous RNA spectrum, which are generated by back-splicing or exon skipping events. Many circRNAs

function critically in carcinogenesis; circ-ITCH, circ-HIPK3, circ-MTO1, and circ-MYLK have been reported to contribute to human BC [9–12], highlighting the importance of circRNAs in BC development. Nevertheless, the biological functions of circRNAs in BC are unclear.

The present study sequenced normal and BC control tissues to determine their circRNA expression profiles. We studied circRGNEF, which was upregulated significantly in BC, and found that downregulation of circRGNEF could suppress BC cell metastasis as well as proliferation via regulation of the miR-548/kinesin family member 2C (KIF2C) axis. Our results provide candidate BC therapeutic targets.

RESULTS

High hsa_circ_0072995 (circRGNEF) expression predicted an unfavorable BC prognosis

To characterize the association between abnormal circRNA expression and BC progression, we performed RNA-Seq analysis for ribosomal RNA-depleted total RNA in four samples of tissue (two BC and two adjacent normal tissues). The data confirmed that circRGNEF expression was significantly increased in BC tissues (Supplementary Materials 1). To survey the role of circRGNEF in BC, we explored circRGNEF expression in BC as well as adjacent normal tissues from 90 BC patients by RT-qPCR. circRGNEF expression was significantly increased in BC tissues (Figure 1A). We used 90 pairs of human BC and adjacent normal tissues to perform circRGNEF FISH assays, which verified that circRGNEF was mainly localized in the cytoplasm (Figure 1B). We also discovered that high circRGNEF expression was correlated with lymph node metastasis, high pathological T stage, and high stage (Table 1). High circRGNEF expression was also correlated with poorer overall survival (Figure 1C) compared to patients with low circRGNEF expression. hsa_circ_0072995 is derived from circularizing two exons of the *RGNEF* gene, which is within the region chr5:73069679–73076570. *RGNEF* consists of 6891 bp and the spliced mature circRNA is 435 bp (Figure 1D); we therefore named hsa_circ_0072995 as circRGNEF.
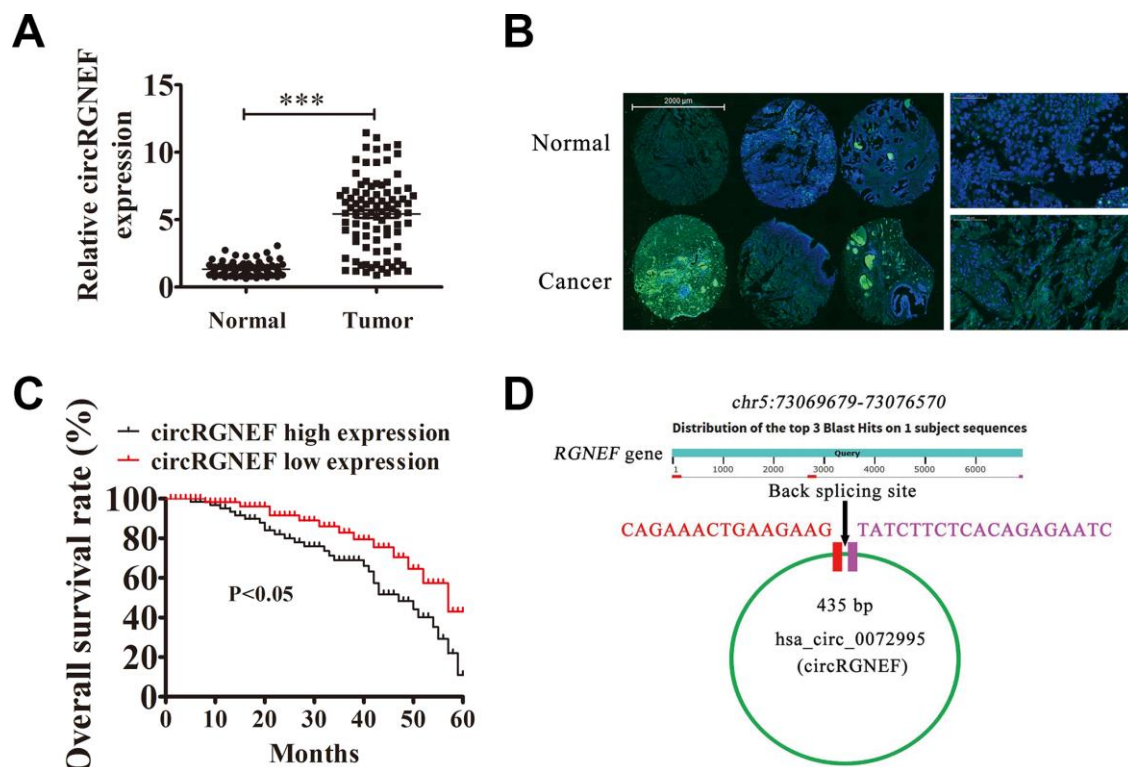

Figure 1. High expression of hsa_circ_0072995 (circRGNEF) predicted an unfavorable prognosis of bladder cancer (BC). (**A**) RT-qPCR assay of circRGNEF in 90 paired BC tumor and adjacent non-tumor tissues. Data are means ± standard deviation (SD). ***$P < 0.001$ vs. normal controls. (**B**) Fluorescent *in situ* hybridization (FISH) indicates the subcellular localization of circRGNEF. (**C**) The prognostic significance of circRGNEF expression for BC patients was performed with FISH values using the median value as the cut-off. The observation time was 60 months. (**D**) Genomic loci of *RGNEF* and circRGNEF. The red signal indicates back splicing.

Table 1. Relationship between the expression levels of circRGNEF and clinicopathological features in bladder cancer.

Characteristics	No. (%)	circRGNEF expression		
		Low (%)	High (%)	*P*-value
Gender				
Male	81 (90.0)	24 (29.6)	57 (70.3)	0.452
Female	9 (10.0)	4 (44.4)	5 (55.6)	
Age				
<65	56 (62.2)	18 (23.8)	38 (76.2)	0.818
≥65	34 (37.8)	10 (37.5)	24(62.5)	
Tumour size				
<3 cm	38 (42.2)	12 (31.6)	26 (68.4)	0.999
≥3 cm	52 (57.8)	16 (30.8)	36 (69.2)	
Pathology stage				
pTa-pT1	44 (48.9)	20 (45.5)	24 (54.5)	0.006
pT2-T4	46 (51.1)	8 (17.4)	38 (82.6)	
Grade				
Low	51 (56.7)	22 (43.1)	29 (56.9)	0.006
High	39 (43.3)	6 (15.4)	33 (84.6)	
Lymphatic metastasis				
Yes	22 (24.4)	2 (9.01)	20 (90.9)	0.015
No	68 (75.6)	26 (38.2)	42 (61.8)	
Muscle invasion				
NMIBC	61 (67.8)	24 (39.3)	37 (60.7)	0.017
MIBC	29 (32.2)	4 (13.8)	25 (86.2)	
Total	90	28	62	

circRGNEF expression in BC cell lines increased and circRGNEF knockdown suppressed cell proliferation *in vitro* and *in vivo*

circRGNEF expression in BC cell lines was increased compared with normal SV-HUC cells (Figure 2A). T24 and UM-UC-3 cells had higher circRGNEF expression, so we used T24 and UM-UC-3 cells for further experiments. We generated a siRNA targeting circRGNEF (si-circRGNEF); circRGNEF expression was decreased significantly compared to the NC group in both UMUC-3 and T24 cells following circRGNEF knockdown (Figure 2B). Cell cycle distribution analysis confirmed that the number of cells in S-phase decreased significantly and the G2/M-phase proportion increased following depletion of circRGNEF (Figure 2C), indicating cell cycle arrest at G2/M. CCK8 (Figure 2D and 2E), colony formation (Figure 2F), and EdU (Figure 2G and 2H) assays showed that downregulation of circRGNEF suppressed cell proliferation in both UMUC-3 and T24 cells. The xenograft results verified that circRGNEF knockdown suppressed T24 tumor weight and volume compared with the NC group (Figure 3A–3C). Immunohistochemical detection with Ki67

staining showed that circRGNEF silencing suppressed Ki67 expression in tumor tissues (Figure 3D), indicating that circRGNEF knockdown suppressed tumor growth.

Knockdown of circRGNEF decreased BC cell invasion *in vivo* and *in vitro*

Invasion and migration analyses by Transwell assay revealed that depletion of circRGNEF decreased T24 and UMUC-3 cell invasion and migration (Figure 4A–4C). T24 cell metastasis was also decreased after circRGNEF silencing, as assessed by live imaging (Figure 4D), suggesting that knockdown of circRGNEF suppresses BC invasion *in vivo* and *in vitro*.

miR-548 and KIF2C are downstream targets of circRGNEF

Several studies have confirmed that circRNAs, including miRNA response elements, can correlate to miRNAs as competitive endogenous RNAs and regulate target mRNA expression [10, 13]. Thus, we selected T24 cells with or without circRGNEF silencing for high-throughput sequencing. circRGNEF depletion
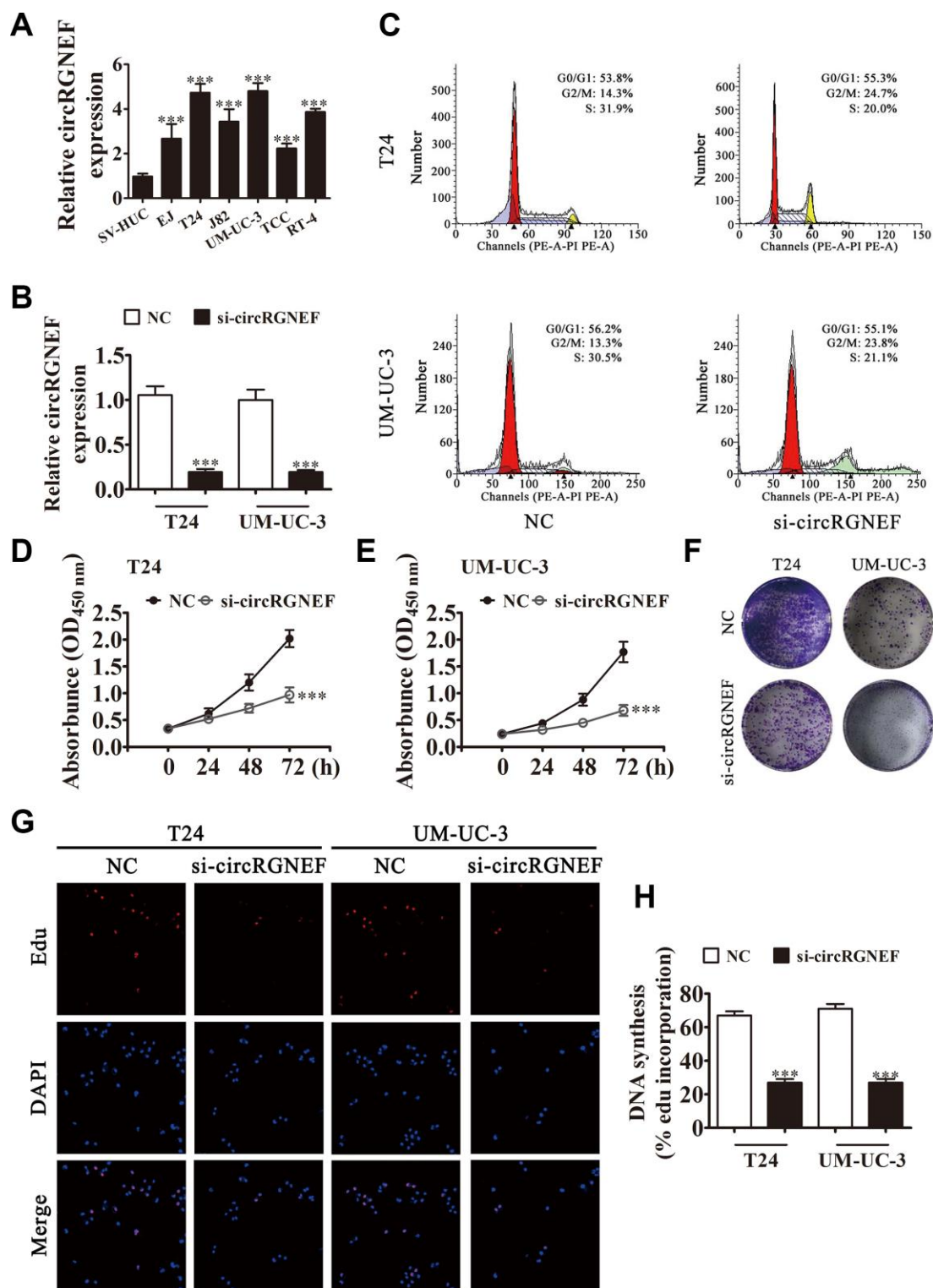
Figure 2. circRGNEF expression was also increased in BC cell lines and knockdown of circRGNEF suppressed cell proliferation. (**A**) RT-qPCR detection of circRGNEF expression in BC cell lines EJ, T24, J82, UM-UC-3, TCC, and RT-4, and the normal cell line SV-HUC. Data are presented as the mean ± SD. ***$P < 0.001$ vs. SV-HUC. (**B**) RT-qPCR detection shows the expression of circRGNEF in both T24 and UM-UC-3 cells following transfection with small interfering RNA targeting circRGNEF (si-circRGNEF) or negative control (NC). Data are presented as the mean ± SD. ***$P < 0.001$ vs. NC. (**C**) Cell cycle distribution by flow cytometry after propidium iodide staining. (**D**, **E**) CCK8 assay shows the proliferation of T24 and UM-UC-3 cells with or without circRGNEF silencing. Data are presented as the mean ± SD. ***$P < 0.001$ vs. NC. (**F**) Colony formation assay was performed to determine the colony-forming ability of T24 and UM-UC-3 cells. (**G**, **H**) circNRIP1 silencing significantly inhibited DNA synthesis, as determined by the EdU assay. Data are presented as the mean ± SD. ***$P < 0.001$ vs. NC.
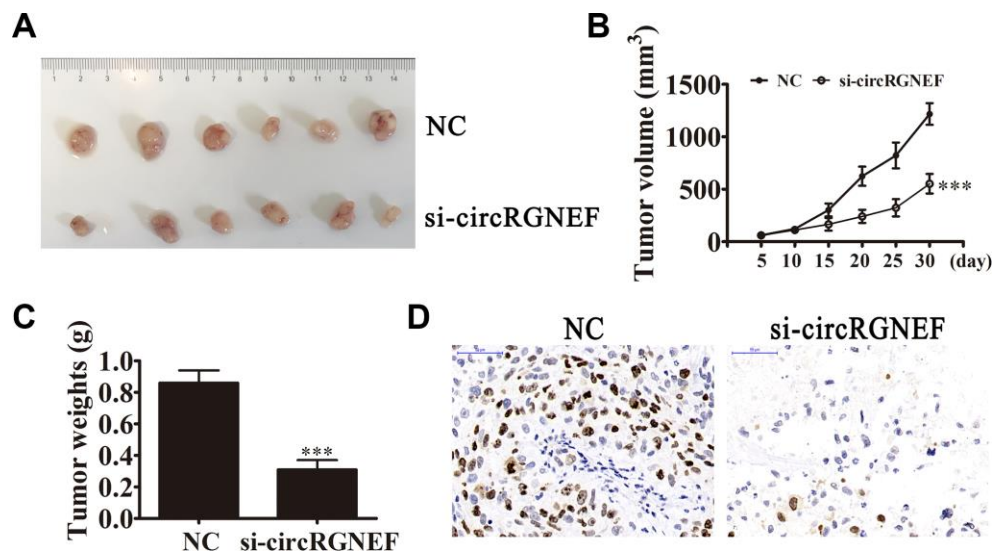
Figure 3. circRGNEF silencing suppressed tumor growth of xenografts in nude mice. (**A**, **B**) Photographs of tumors and curve of T24 tumor volume growth (**B**) of the nude mice. Data are presented as the mean ± SD. ***$P < 0.001$ vs. NC. (**C**) Tumor weights. Data are presented as the mean ± SD. ***$P < 0.001$ vs. NC. (**D**) Ki67 staining of tumor tissues.
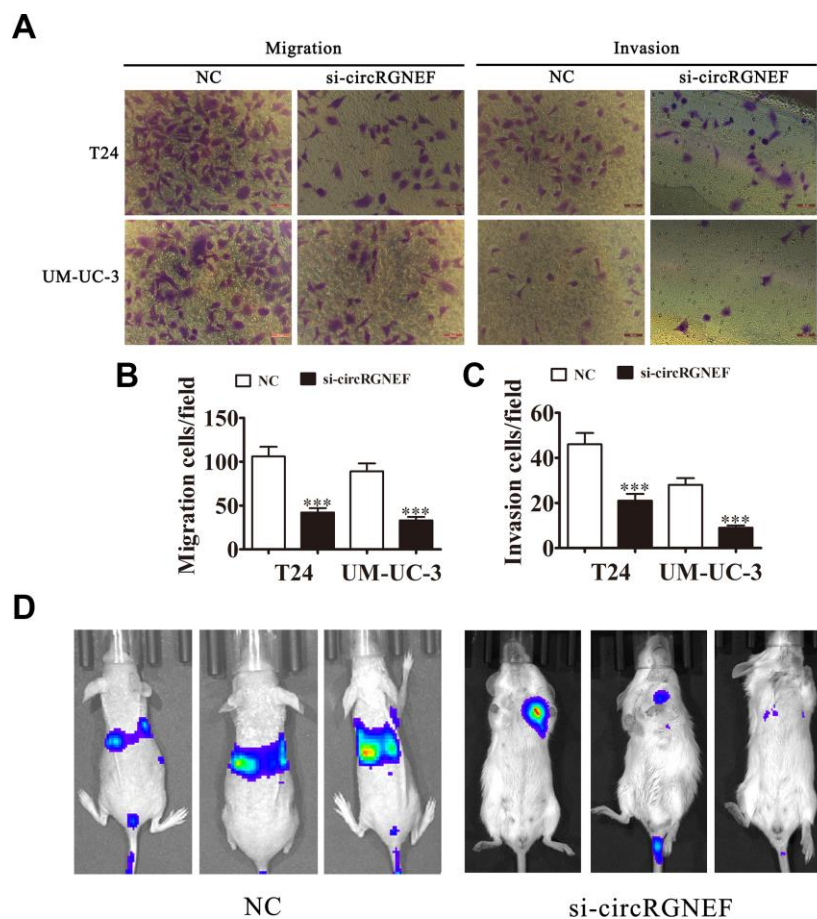

Figure 4. Knockdown of circRGNEF decreased the invasion ability of BC *in vitro* and *in vivo*. (**A**–**C**) Cell migration and invasion were assessed in T24 and UM-UC-3 cells using Transwell assays. Data are presented as the mean ± SD. ***$P < 0.001$ vs. NC. (**D**) Live imaging shows the effects of circRGNEF on metastasis of T24 cells 30 days after intravenous tail injection.

resulted in upregulation of a number of miRNAs (Supplementary Materials 2). Combined with the biological analysis, these results infer that miR-548 is a circRGNEF target (Figure 5A). RR-qPCR revealed that miR-548 expression was decreased in BC and adjacent normal tissues of 90 BC patients (Figure 5B).

Bioinformatics analyses indicated that miR-548 is a downstream target of circRGNEF. To verify the relationship between circRGNEF and miR-548, we inserted WT or Mut circRGNEF sequences including the miR-548 binding sequence into luciferase reporter vectors (Figure 5C). We then transfected the luciferase
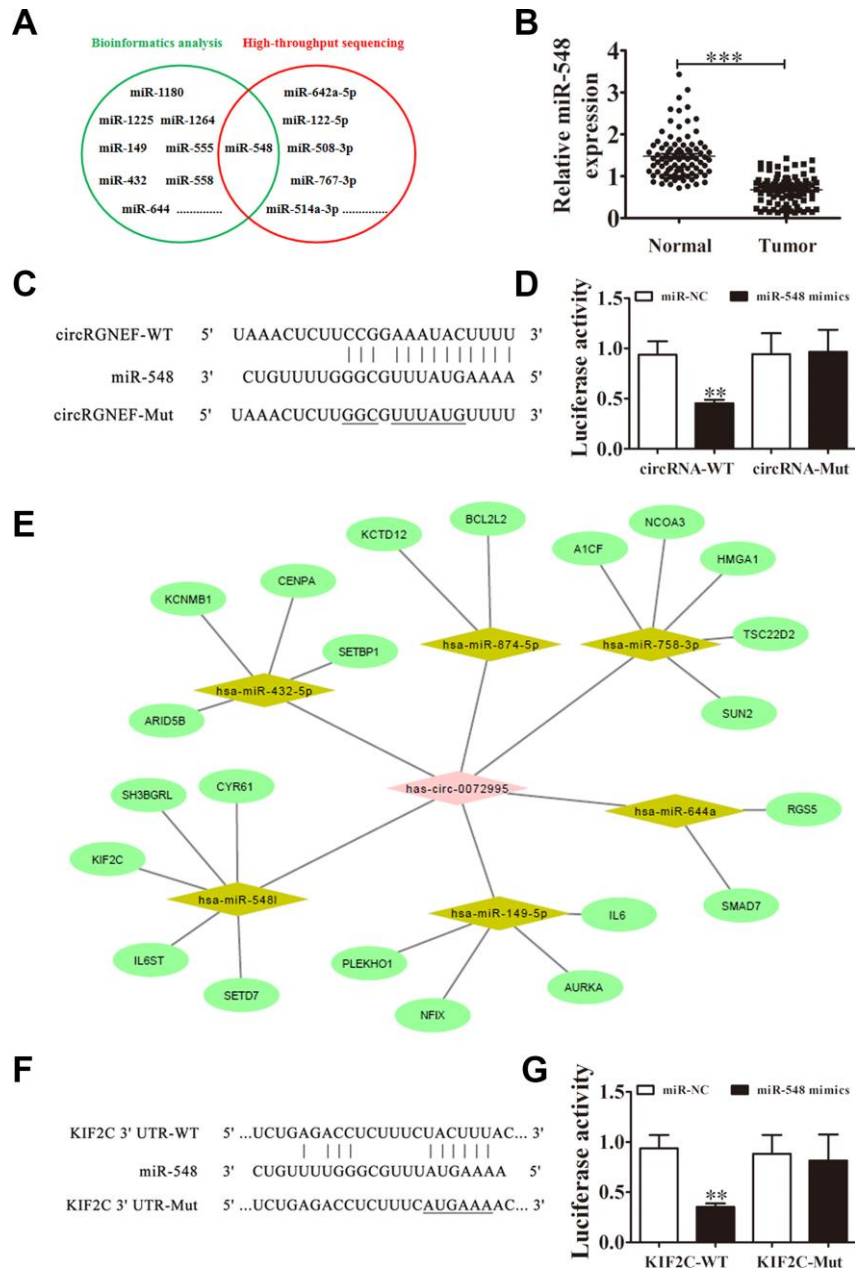

Figure 5. miR-548 and KIF2C are downstream targets of circRGNEF. (**A**) Bioinformatics analysis (https://circinteractome.nia.nih.gov/bin/mirnasearch) and high-throughput sequencing indicated miR-548 is a target of circRGNEF. (**B**) RT-qPCR assay of miR-548 in 90 paired BC tumor and adjacent non-tumor tissues. Data are means ± SD. ***$P < 0.001$ vs. normal controls. (**C**) The mutated (Mut) version of circRGNEF is shown. (**D**) The relative luciferase activity was determined 48 h after transfection of HEK293T cells with miR-548 mimic/normal control (NC) or circRGNEF wild-type/Mut. Data are presented as the mean ± SD. ***$P < 0.001$. (**E**) Bioinformatics analysis (http://circnet.mbc.nctu.edu.tw/ and http://www.targetscan.org/vert_71/) indicated KIF2C is a direct target of miR-548. (**F**) The mutated (Mut) version of the 3'UTR-KIF2C is shown. (**G**) The relative luciferase activity was determined 48 h after transfection of HEK293T cells with miR-548 mimic/normal control (NC) or 3'UTR-KIF2C wild-type/Mut. Data are presented as the mean ± SD. ***$P < 0.001$.

reporter vectors into HEK293T cells in the presence or absence of miR-548 mimic. Luciferase reporter analyses showed that miR-638 inhibited luciferase activity in WT cells though not in Mut cells (Figure 5D), indicating that miR-548 is a target of circRGNEF.

Bioinformatics analyses also suggested that KIF2C is a downstream target of miR-548 (Figure 5E). To validate the relationship between KIF2C and miR-548, we inserted WT or Mut 3'UTR-KIF2C sequences including the miR-548 binding sequence into luciferase reporter vectors (Figure 5F). We then transfected the luciferase reporter vectors into HEK293T cells in the presence or absence of miR-548 mimic. Luciferase reporter analysis suggested that miR-548 inhibited luciferase activity in WT cells while not in Mut cells (Figure 5G), indicating that KIF2C is a target of miR-548.

miR-548 downregulation or KIF2C overexpression restored proliferation, migration, and invasion after circRGNEF silencing

RT-qPCR analysis showed that circRGNEF silencing suppressed circRGNEF and KIF2C expression, but promoted miR-548 expression. When combined with treatment with miR-548 inhibitor, miR-548 expression was suppressed and KIF2C expression was restored. miR-548 inhibitor had no effect on circRGNEF expression. Following transfection with a KIF2C overexpression vector, KIF2C expression increased significantly in UMUC-3 and T24 cells but there was no change in the expression of circRGNEF and miR-548 (Figure 6A–6F), suggesting that miR-548 and KIF2C are downstream targets of circRGNEF. DNA synthesis assessed by EdU assay revealed that miR-548 downregulation or KIF2C overexpression restored proliferation of both T24 and UMUC-3 cells after circRGNEF silencing (Figure 6G–6I). Analysis of migration and invasion showed that downregulation of miR-548 or overexpression of KIF2C restored invasion and migration abilities in both UMUC-3 and T24 cells after circRGNEF silencing (Figure 6J–6N).

KIF2C overexpression reversed miR-548-induced cell invasion, migration, and growth inhibition *in vitro*

To validate the relationship between miR-548 and KIF2C, we constructed miR-548-overexpressing cells in the presence or absence of KIF2C overexpression. miR-548 expression was increased in T24 and UMUC-3 cells together with transfection of the miR-548 mimic. However, KIF2C overexpression had no effect on miR-548 expression (Figure 7A and 7B). The results also showed that miR-548 overexpression decreased KIF2C expression in UMUC-3 cells following transfection with miR-548 mimic. But KIF2C overexpression significantly promoted KIF2C expression because heterogeneous transfection of KIF2C with no 3'UTR cannot interact with and be degraded by miR-548 (Figure 7C and 7D), suggesting that KIF2C is a downstream target of miR-548.

The EdU assay verified that miR-548 upregulation suppressed T24 and UMUC-3 cell proliferation whereas overexpression of KIF2C restored T24 and UMUC-3 cell proliferation after miR-548 overexpression (Figure 7E–7H). Transwell assays showed that overexpression of KIF2C restored invasion and migration abilities in T24 and UMUC-3 cells following miR-548 overexpression (Figure 7I–7M).

DISCUSSION

An increasing number of studies have found that the expression of non-coding RNAs, i.e., circRNAs, long non-coding RNAs, and miRNAs, are abnormal in various cancers. Previous investigations have focused on their epigenetic regulation during cancer development [14, 15]. circRNAs compose a large population of noncoding RNAs derived from various genomic locations and are expressed in tissue-, cell type-, and developmental stage-specific manners. Due to their covalent loop structure without 5' caps or 3' polyadenylated tails, circRNAs are difficult to reverse transcribe with oligo-dT primers and are more stable than linear mRNAs, which gives them specific advantages as cancer biomarkers. The present study suggested that circRGNEF expression was increased significantly in both BC cell lines and tissues. High circRGNEF expression was correlated with high stage, lymph node metastasis, and high pathological T stage. We also found that high circRGNEF expression predicted poorer overall survival. Thus, high circRGNEF expression functions in BC progression. To uncover the regulatory mechanism, we generated si-circRGNEF and found that circRGNEF downregulation suppressed migration, proliferation, and invasion *in vivo* and *in vitro*. The role of non-coding circRNAs as candidate miRNA "sponges" has been recognized [16–18]. In this research, bioinformatics analysis and high-throughput sequencing revealed that miR-548 is a target of circRGNEF; this was verified by luciferase reporter assay.

Previous investigations have found that miR-548 has 69 genes that located in nearly all the chromosomes, which is a super primate-specific miRNA gene family [19]. Due to its alignment with the hepatitis C virus, HIV-1, and hepatitis B virus [20], miR-548 is a target for the development of novel antiviral therapeutics. Some investigations have also shown that miR-548 might
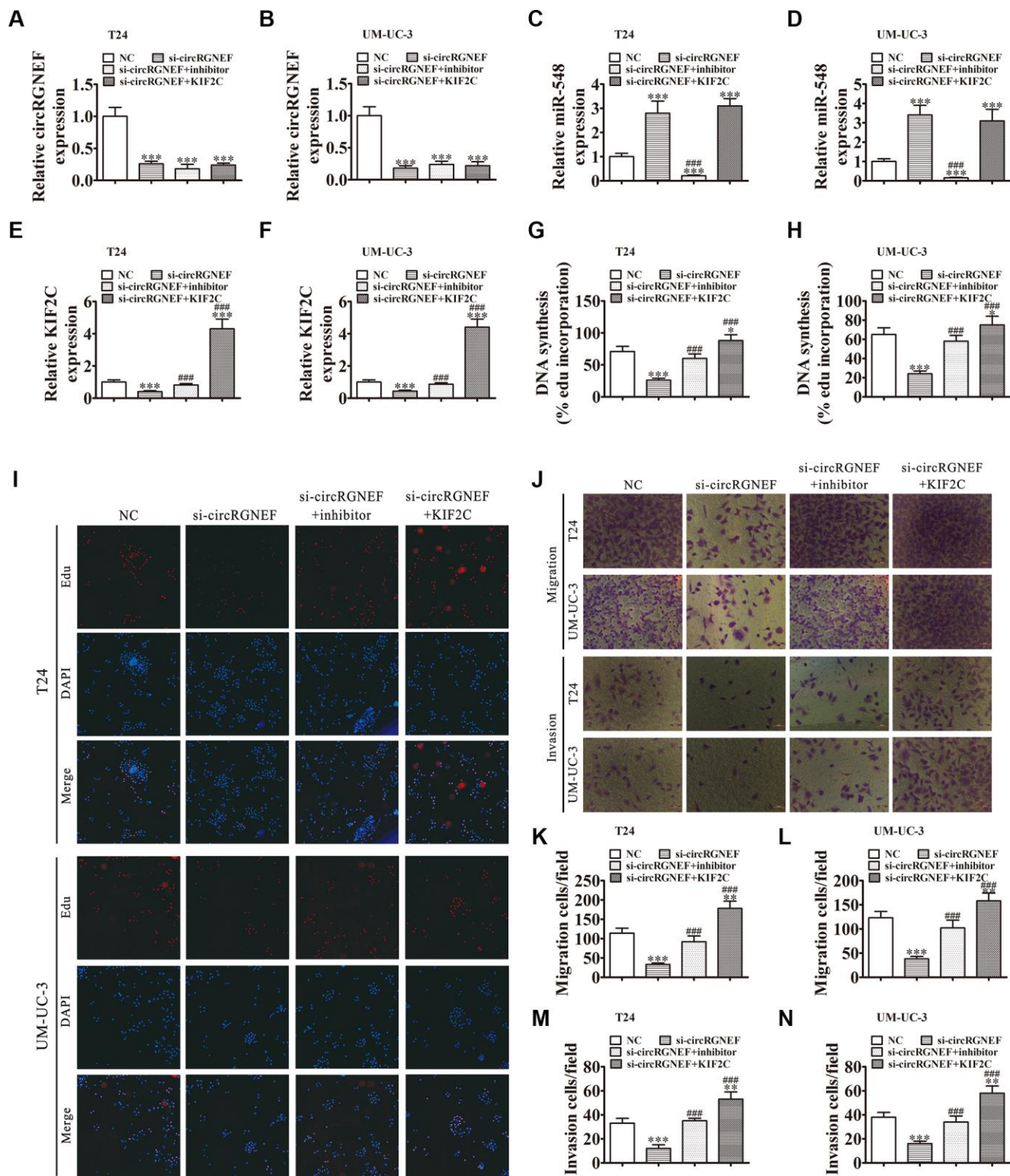
Figure 6. Downregulation of miR-548 or overexpression of KIF2C restored proliferation, migration, and invasion after circRGNEF silencing. (**A–F**) RT-qPCR shows the expression of circRGNEF (**A**, **B**), miR-548 (**C**, **D**), and KIF2C (**E**, **F**) in T24 and UM-UC-3 cells following transfection or treatment with NC, si-circRGNEF, miR-548 inhibitor, KIF2C overexpression vector (KIF2C) single or combined. Data are presented as the mean ± SD. ***$P < 0.001$ vs. NC. ###$P < 0.001$ vs. si-circRGNEF. (**G–I**) Cell proliferation was analyzed by EdU assays. Data are presented as the mean ± SD. ***$P < 0.001$ vs. NC. ###$P < 0.001$ vs. si-circRGNEF. (**J–N**) Cell migration and invasion were assessed in T24 and UM-UC-3 cells using Transwell assays. Data are presented as the mean ± SD. ***$P < 0.001$ vs. NC. ###$P < 0.001$ vs. si-circRGNEF.

function in different types of cancer, including prostate cancer, breast cancer, and pancreatic cancer [21–24]. This study discovered that miR-548 expression was decreased in BC tissues. circRGNEF downregulation promoted miR-548 expression and miR-548 silencing restored migration, proliferation, and invasion following circRGNEF knockdown. miR-548 overexpression suppressed BC cell migration, proliferation, and invasion, which is consistent with previous studies [25, 26].

Bioinformatics analyses revealed that KIF2C is a miR-548 target, which was validated by luciferase reporter assay. *In vitro* experiments revealed that miR-548 overexpression suppressed BC cell metastasis and
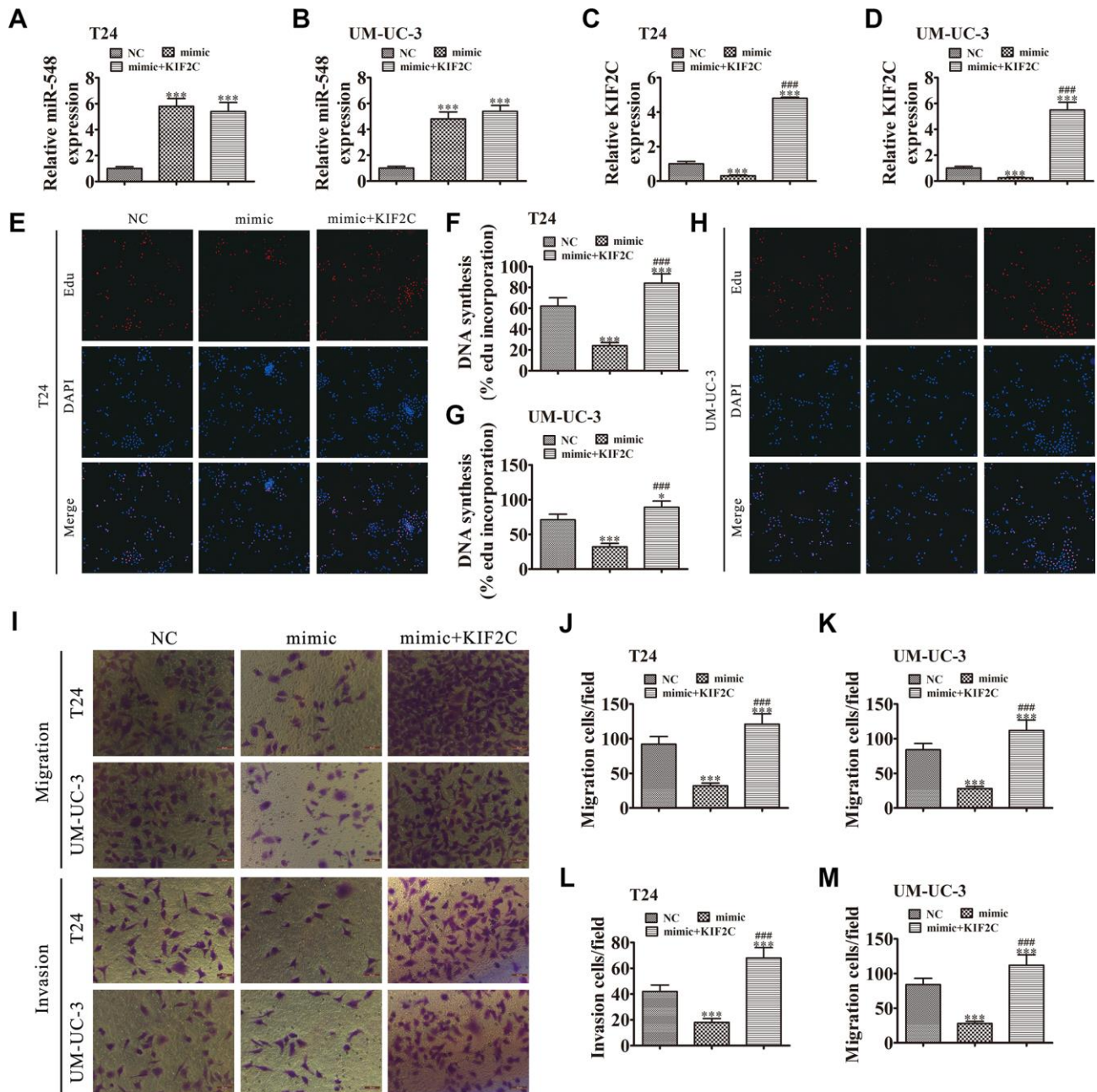

Figure 7. KIF2C overexpression reversed miR-548-induced cell migration, invasion, and growth inhibition *in vitro*. (**A**–**D**) T24 and UM-UC-3 cells were transfected with miR-548 mimics with or without the KIF2C overexpression vector. RT-qPCR shows the expression of miR-548 (**A**, **B**) and KIF2C (**C**, **D**) in T24 and UM-UC-3 cells. Data are denoted by the mean ± SD. ***$P < 0.001$ vs. NC. ###$P < 0.001$ vs. mimic. (**E**–**H**) EdU assay showing the proliferation of T24 (**E**, **F**) and UM-UC-3 (**G**, **H**) cells. Data are denoted by the mean ± SD. *$P < 0.05$, ***$P < 0.001$. ###$P < 0.001$ vs. mimic. (**I**–**M**) Cell migration and invasion were determined in T24 and UM-UC-3 cells by Transwell assays. Data are denoted by the mean ± SD. ***$P < 0.001$ vs. NC. ###$P < 0.001$ vs. mimic.

proliferation by suppressing KIF2C expression. KIF2C overexpression decreased BC cell metastasis and proliferation following miR-548 overexpression since heterologous KIF2C has no 3'-UTR. In this manner, miR-548 could not interact with the KIF2C 3'UTR and silence it at the mRNA level. KIF2C is a mitotic centromere-associated kinesin; the role of KIF2C has been extensively characterized [27]. KIF2C localizes to the cytoplasm throughout the cell cycle, and is specifically localized at centromeres/kinetochores, centrosomes, and the spindle midzone in mitosis [28, 29]. Many studies have indicated that KIF2C expression likely functions in cancer progression and development, including esophageal squamous cell carcinoma [30], non-small cell lung cancer [31], and gliomas [32]. The present study showed that circRGNEF downregulation decreased KIF2C expression. miR-548 downregulation or KIF2C overexpression restored proliferation, migration, and invasion abilities after circRGNEF silencing, suggesting that circRGNEF promotes BC progression via miR-548/KIF2C axis regulation.

CONCLUSIONS

In conclusion, our study found that the increase in circRGNEF expression in BC is closely related to BC development and occurrence. We have shown that circRGNEF directly targets miR-548 through upregulation of KIF2C expression. Downregulation of circRGNEF suppressed BC progression by promoting miR-548 and decreasing KIF2C expression. This provides us with a potential prognostic and therapeutic target for circRGNEF in BC treatment.

MATERIALS AND METHODS

Animal ethics statement

We used 12 BALB/c nude mice aged 4 weeks and weighing 15~20 g (SLARC, Shanghai, China) in the present study. Ethics Committee in Huashan Hospital, Fudan University approved animal experiments.

Patients and samples

In total, we collected 90 pairs of BC and adjacent normal tissues from BC patients enrolled in Huashan Hospital, Fudan University from January 2007 to January 2013. No patients received preoperative local or systemic treatment in prior specimen collection. We acquired informed consent from patients or patients' relatives. Ethics Committee at Huashan Hospital, Fudan University approved this project. We directly deposited collected tissues in liquid nitrogen and 4% paraformaldehyde for further use.

High-throughput RNA-Seq and strand-specific RNA-Seq library construction

We extracted total RNA from two pairs of BC and adjacent noncancerous tissues or T24 cells with or without small interfering RNA targeting circRGNEF (si-circRGNEF) via TRIzol reagent (Invitrogen, Carlsbad, CA, USA). We subjected nearly 3 μg of total RNA from every sample to VAHTS Total RNA-seq (H/M/R) Library Prep Kit for Illumina (Vazyme Biotech Co., Ltd, Nanjing, China) to eliminate ribosomal RNA. We retained other RNA such as non-coding RNA and mRNA. We treated purified RNA with RNase R (Epicenter, 40 U, 37°C for 3 h), and then performed TRIzol purification. We prepared RNA-Seq libraries through the KAPA Stranded RNA-Seq Library Prep Kit (Roche, Basel, Switzerland), which were subjected to deep sequencing through Illumina HiSeq 4000 at Aksomics, Inc., Shanghai, China (accession number: H1712024).

Cell culture and transfection

We obtained SV-HUC and BC (J82, EJ, T24, TCC, UM-UC-3, and RT-4) cell lines from Type Culture Collection (Shanghai, China) in Chinese Academy of Sciences. Cells were culturedin Dulbecco's modified Eagle medium (DMEM; Gibco, Grand Island, NY, USA) with 10% fetal bovine serum (FBS) at 37°C in a humidified incubator with 5% CO_2.

We transfected si-circRGNEF, miR-548 inhibitors, miR-548 mimics, KIF2C overexpression vector, and respective negative controls into cultured UM-UC-3 and T24 cells using Lipofectamine 2000 (Invitrogen) following standard procedure. To further verify the effects of circRGNEF *in vivo*, we constructed lentiviral stabilized circRGNEF-silenced T24 cells.

Bioinformatics analyses

We predicted circRNA/miRNA target genes via the web-based tool *Circular RNA Interactome*. We predicted correlations between KIF2C and miR-548 through *TargetScanHuman* and the http://circnet.mbc.nctu.edu.tw/ website.

Colony formation and cell proliferation assays

We used Cell Counting Kit-8 (CCK-8; Gibco) assay to assess cell viability. We seeded transfected cells into 96-well plates at a density of 2000 cells per well in triplicate wells. We detected cell viability at 0, 24, 48, and 72 h after seeding according to standard procedure.

For the colony formation assay, we seeded transfected cells into 6-well plates at a density of 2000 cells per well. Cells were maintained in DMEM medium containing 10% FBS for 10 days. We fixed and stained samples, and counted and imaged colonies.

5-Ethynyl-2′-deoxyuridine (EdU) assay

We used the EdU assay kit (RiboBio, China) to assess cell proliferation and DNA synthesis. We cultured 10,000 treated PC cells in a 96-well plate overnight. The following day, we added EdU solution (25 μM) and incubated cells for 1 day. We then fixed cells with 4% formalin at room temperature for 2 h. Afterwards, 0.5% Triton X-100 was applied for 10 min to permeabilize the cells and Apollo reaction solution (200 μL) was added to stain EdU for 30 min and 4,6-diamidino-2-phenylindole (DAPI; 200 μL) to stain nuclei. Lastly, a Nikon microscope (Nikon, Japan) was used to detect proliferation and DNA synthesis, reflected by blue and red signals, respectively.

Fluorescence in situ hybridization (FISH)

We prepared specific probes to circRGNEF (Dig-5′ - AAACTGAAGAAGTATCTTCTCACAGAG -3′-Dig) (Geneseed Biotech, Guangzhou, China). We detected signals using FITC-conjugated anti-biotin antibodies (Jackson ImmunoResearch Inc., West Grove, PA, USA). We counterstained cell nuclei with DAPI. We obtained images using Zeiss LSM 700 confocal microscope (Carl Zeiss, Oberkochen, Germany).

Migration and invasion assay

We measured cell invasion and migration using a BD Transwell chamber with 24 wells (Costar, Boston, MA, USA), uncoated or pre-coated with Matrigel, following the standard procedure. We seeded cells (6×10^4 cells per well for migration; 8×10^4 cells per well for invasion) in 500 μl serum-free medium to the insert, and placed media supplemented with 10% FBS as a chemoattractant in the lower chamber. After incubation at 37°C for 1 day, we fixed and stained the invaded cells at the lower surface of the insert with 1% crystal violet. We then counted and imaged cells.

RT-qPCR

We conducted RNA extraction using TRIzol reagent (Invitrogen) as previously described [33]. We obtained cDNA using a pTRUEscript 1st Strand cDNA Synthesis Kit (Aidlab, Beijing, China). We conducted RT-qPCR with the 2× SYBR Green qPCR Mix (Aidlab) on the ABI 7900HT sequence detection machine (Thermo Fisher Scientific, Waltham, MA,

USA). Expression fold differences were determined via the $2^{-\Delta\Delta CT}$ method.

Luciferase reporter assay

We amplified wild type (WT) cDNA fragments of circRGNEF or the KIF2C 3' untranslated region (UTR) including predicted miR-548 binding sites and generated mutated (Mut) fragments by overlap extension PCR. We cloned WT and Mut fragments into psiCHECK-2 (Promega, Madison, WI, USA). For the luciferase reporter assay, we co-transfected HEK293T cells with WT or Mut vector and miR-548 or control mimics using Lipofectamine 2000 (Thermo Fisher Scientific). After 2 days of transfection, we detected luciferase activity through the dual-luciferase reporter assay kit (Promega) followed by normalization with Renilla luciferase activity. Experiments were performed in triplicate.

Metastasis assays and tumor xenograft formation

We injected 2×10^7 viable cells from negative control (NC) or si-circRGNEF T24 cells into nude mice right flanks as previously described [34]. We measured tumor sizes every 5 days through a vernier caliper. We calculated tumor volume by the equation: volume = length × width^2 × 0.5. Mice were euthanized for qRT-PCR analysis 1 month after implantation.

For metastasis analyses, we transfected T24 cells with luciferase expression vectors into both NC- and si-circRGNEF-silenced cells (2×10^5). We intravenously injected cells into mice tails. After 1 month, we analyzed T24 cell metastasis by bioluminescence imaging with intravenous luciferin injection (150 mg luciferin/kg body weight) into tails of mice.

Statistical analysis

We denoted data by mean ± standard deviation. We used GraphPad Prism (GraphPad, La Jolla, CA, USA) to calculate group differences. $P \leq 0.05$ inferred a statistical significance.

Ethics approval and consent to participate

Huashan Hospital Fudan University Committee approved the present study.

AUTHOR CONTRIBUTIONS

YC, XJ, and JH designed the study. YC, TF, and LQ performed the assays and collected samples. YF and ZZ conducted statistical analyses. YC, CX, MZ, and JS participated in the research coordination and worked as

technical consultants. YC drafted the manuscript. All authors reviewed and contributed to the final manuscript.

CONFLICTS OF INTEREST

Authors declare no conflicts of interest.

FUNDING

REFERENCES

1. Massari F, Ciccarese C, Santoni M, Iacovelli R, Mazzucchelli R, Piva F, Scarpelli M, Berardi R, Tortora G, Lopez-Beltran A, Cheng L, Montironi R. Metabolic phenotype of bladder cancer. Cancer Treat Rev. 2016; 45:46–57.
https://doi.org/10.1016/j.ctrv.2016.03.005
PMID:26975021

2. Antoni S, Ferlay J, Soerjomataram I, Znaor A, Jemal A, Bray F. Bladder Cancer Incidence and Mortality: A Global Overview and Recent Trends. Eur Urol. 2017; 71:96–108.
https://doi.org/10.1016/j.eururo.2016.06.010
PMID:27370177

3. Cumberbatch MG, Jubber I, Black PC, Esperto F, Figueroa JD, Kamat AM, Kiemeney L, Lotan Y, Pang K, Silverman DT, Znaor A, Catto JW. Epidemiology of Bladder Cancer: A Systematic Review and Contemporary Update of Risk Factors in 2018. Eur Urol. 2018; 74:784–95.
https://doi.org/10.1016/j.eururo.2018.09.001
PMID:30268659

4. Kamat AM, Hahn NM, Efstathiou JA, Lerner SP, Malmström PU, Choi W, Guo CC, Lotan Y, Kassouf W. Bladder cancer. Lancet. 2016; 388:2796–810.
https://doi.org/10.1016/S0140-6736(16)30512-8
PMID:27345655

5. Funt SA, Rosenberg JE. Systemic, perioperative management of muscle-invasive bladder cancer and future horizons. Nat Rev Clin Oncol. 2017; 14:221–34.
https://doi.org/10.1038/nrclinonc.2016.188
PMID:27874062

6. Sargos P, Baumann BC, Eapen L, Christodouleas J, Bahl A, Murthy V, Efstathiou J, Fonteyne V, Ballas L, Zaghloul M, Roubaud G, Orré M, Larré S. Risk factors for loco-regional recurrence after radical cystectomy of muscle-invasive bladder cancer: A systematic-review and framework for adjuvant radiotherapy. Cancer Treat Rev. 2018; 70:88–97.
https://doi.org/10.1016/j.ctrv.2018.07.011
PMID:30125800

7. Sanger HL, Klotz G, Riesner D, Gross HJ, Kleinschmidt AK. Viroids are single-stranded covalently closed circular RNA molecules existing as highly base-paired rod-like structures. Proc Natl Acad Sci USA. 1976; 73:3852–56.
https://doi.org/10.1073/pnas.73.11.3852
PMID:1069269

8. Xie Y, Shao Y, Sun W, Ye G, Zhang X, Xiao B, Guo J. Downregulated expression of hsa_circ_0074362 in gastric cancer and its potential diagnostic values. Biomark Med. 2018; 12:11–20.
https://doi.org/10.2217/bmm-2017-0114
PMID:29240459

9. Yang C, Yuan W, Yang X, Li P, Wang J, Han J, Tao J, Li P, Yang H, Lv Q, Zhang W. Circular RNA circ-ITCH inhibits bladder cancer progression by sponging miR-17/miR-224 and regulating p21, PTEN expression. Mol Cancer. 2018; 17:19.
https://doi.org/10.1186/s12943-018-0771-7
PMID:29386015

10. Li Y, Zheng F, Xiao X, Xie F, Tao D, Huang C, Liu D, Wang M, Wang L, Zeng F, Jiang G. CircHIPK3 sponges miR-558 to suppress heparanase expression in bladder cancer cells. EMBO Rep. 2017; 18:1646–59.
https://doi.org/10.15252/embr.201643581
PMID:28794202

11. Zhong Z, Huang M, Lv M, He Y, Duan C, Zhang L, Chen J. Circular RNA MYLK as a competing endogenous RNA promotes bladder cancer progression through modulating VEGFA/VEGFR2 signaling pathway. Cancer Lett. 2017; 403:305–17.
https://doi.org/10.1016/j.canlet.2017.06.027
PMID:28687357

12. Li Y, Wan B, Liu L, Zhou L, Zeng Q. Circular RNA circMTO1 suppresses bladder cancer metastasis by sponging miR-221 and inhibiting epithelial-to-mesenchymal transition. Biochem Biophys Res Commun. 2019; 508:991–96.
https://doi.org/10.1016/j.bbrc.2018.12.046
PMID:30551873

13. Liu S, Li X, Lin Z, Su L, Yan S, Zhao B, Miao J. SEC-induced activation of ANXA7 GTPase suppresses prostate cancer metastasis. Cancer Lett. 2018; 416:11–23.
https://doi.org/10.1016/j.canlet.2017.12.008
PMID:29247827

14. Lu Q, Liu T, Feng H, Yang R, Zhao X, Chen W, Jiang B, Qin H, Guo X, Liu M, Li L, Guo H. Circular RNA circSLC8A1 acts as a sponge of miR-130b/miR-494 in suppressing bladder cancer progression via regulating PTEN. Mol Cancer. 2019; 18:111.

https://doi.org/10.1186/s12943-019-1040-0
PMID:31228937

15. Dong W, Bi J, Liu H, Yan D, He Q, Zhou Q, Wang Q, Xie R, Su Y, Yang M, Lin T, Huang J. Circular RNA ACVR2A suppresses bladder cancer cells proliferation and metastasis through miR-626/EYA4 axis. Mol Cancer. 2019; 18:95.
https://doi.org/10.1186/s12943-019-1025-z
PMID:31101108

16. Li W, Li Y, Sun Z, Zhou J, Cao Y, Ma W, Xie K, Yan X. Comprehensive circular RNA profiling reveals the regulatory role of the hsa_circ_0137606/miR-1231 pathway in bladder cancer progression. Int J Mol Med. 2019; 44:1719–28.
https://doi.org/10.3892/ijmm.2019.4340
PMID:31545480

17. Su H, Tao T, Yang Z, Kang X, Zhang X, Kang D, Wu S, Li C. Circular RNA cTFRC acts as the sponge of MicroRNA-107 to promote bladder carcinoma progression. Mol Cancer. 2019; 18:27.
https://doi.org/10.1186/s12943-019-0951-0
PMID:30782157

18. Zhang X, Wang S, Wang H, Cao J, Huang X, Chen Z, Xu P, Sun G, Xu J, Lv J, Xu Z. Circular RNA circNRIP1 acts as a microRNA-149-5p sponge to promote gastric cancer progression via the AKT1/mTOR pathway. Mol Cancer. 2019; 18:20.
https://doi.org/10.1186/s12943-018-0935-5
PMID:30717751

19. Liang T, Guo L, Liu C. Genome-wide analysis of mir-548 gene family reveals evolutionary and functional implications. J Biomed Biotechnol. 2012; 2012:679563.
https://doi.org/10.1155/2012/679563 PMID:23091353

20. Xing TJ, Xu HT, Yu WQ, Wang B, Zhang J. MiRNA-548ah, a potential molecule associated with transition from immune tolerance to immune activation of chronic hepatitis B. Int J Mol Sci. 2014; 15:14411–26.
https://doi.org/10.3390/ijms150814411
PMID:25196343

21. Hu B, Ying X, Wang J, Piriyapongsa J, Jordan IK, Sheng J, Yu F, Zhao P, Li Y, Wang H, Ng WL, Hu S, Wang X, et al. Identification of a tumor-suppressive human-specific microRNA within the FHIT tumor-suppressor gene. Cancer Res. 2014; 74:2283–94.
https://doi.org/10.1158/0008-5472.CAN-13-3279
PMID:24556720

22. Ke H, Zhao L, Feng X, Xu H, Zou L, Yang Q, Su X, Peng L, Jiao B. NEAT1 is Required for Survival of Breast Cancer Cells Through FUS and miR-548. Gene Regul Syst Bio. 2016 (Suppl 1); 10:11–17.
https://doi.org/10.4137/GRSB.S29414
PMID:27147820

23. Saffari M, Ghaderian SM, Omrani MD, Afsharpad M, Shankaie K, Samadaian N. The Association of miR-let 7b and miR-548 with PTEN in Prostate Cancer. Urol J. 2019; 16:267–73.
https://doi.org/10.22037/uj.v0i0.4564
PMID:30318571

24. Zhu S, He C, Deng S, Li X, Cui S, Zeng Z, Liu M, Zhao S, Chen J, Jin Y, Chen H, Deng S, Liu Y, et al. MiR-548an, Transcriptionally Downregulated by HIF1α/HDAC1, Suppresses Tumorigenesis of Pancreatic Cancer by Targeting Vimentin Expression. Mol Cancer Ther. 2016; 15:2209–19.
https://doi.org/10.1158/1535-7163.MCT-15-0877
PMID:27353169

25. Shi Y, Qiu M, Wu Y, Hai L. MiR-548-3p functions as an anti-oncogenic regulator in breast cancer. Biomed Pharmacother. 2015; 75:111–16.
https://doi.org/10.1016/j.biopha.2015.07.027
PMID:26297544

26. Habieb A, Matboli M, El-Tayeb H, El-Asmar F. Correction to: potential role of lncRNA-TSIX, miR-548-a-3p, and SOGA1 mRNA in the diagnosis of hepatocellular carcinoma. Mol Biol Rep. 2019; 46:4591.
https://doi.org/10.1007/s11033-019-04838-z
PMID:31049832

27. Wordeman L, Mitchison TJ. Identification and partial characterization of mitotic centromere-associated kinesin, a kinesin-related protein that associates with centromeres during mitosis. J Cell Biol. 1995; 128:95–104.
https://doi.org/10.1083/jcb.128.1.95 PMID:7822426

28. Walczak CE, Mitchison TJ, Desai A. XKCM1: a Xenopus kinesin-related protein that regulates microtubule dynamics during mitotic spindle assembly. Cell. 1996; 84:37–47.
https://doi.org/10.1016/S0092-8674(00)80991-5
PMID:8548824

29. Maney T, Hunter AW, Wagenbach M, Wordeman L. Mitotic centromere-associated kinesin is important for anaphase chromosome segregation. J Cell Biol. 1998; 142:787–801.
https://doi.org/10.1083/jcb.142.3.787
PMID:9700166

30. Duan H, Zhang X, Wang FX, Cai MY, Ma GW, Yang H, Fu JH, Tan ZH, Fu XY, Ma QL, Wang XY, Lin P. KIF-2C expression is correlated with poor prognosis of operable esophageal squamous cell carcinoma male patients. Oncotarget. 2016; 7:80493–507.
https://doi.org/10.18632/oncotarget.11492
PMID:27563815

31. Gan H, Lin L, Hu N, Yang Y, Gao Y, Pei Y, Chen K, Sun B. KIF2C exerts an oncogenic role in nonsmall cell lung

cancer and is negatively regulated by miR-325-3p. Cell Biochem Funct. 2019; 37:424–31.
https://doi.org/10.1002/cbf.3420
PMID:31328811

32. Bie L, Zhao G, Wang YP, Zhang B. Kinesin family member 2C (KIF2C/MCAK) is a novel marker for prognosis in human gliomas. Clin Neurol Neurosurg. 2012; 114:356–60.
https://doi.org/10.1016/j.clineuro.2011.11.005
PMID:22130050

33. Wang C, Tao W, Ni S, Chen Q. Circular RNA *circ-Foxo3* induced cell apoptosis in urothelial carcinoma via interaction with *miR-191-5p.* Onco Targets Ther. 2019; 12:8085–94.
https://doi.org/10.2147/OTT.S215823
PMID:31802888

34. Yang D, Du G, Xu A, Xi X, Li D. Expression of miR-149-3p inhibits proliferation, migration, and invasion of bladder cancer by targeting S100A4. Am J Cancer Res. 2017; 7:2209–19.
PMID:29218245

SUPPLEMENTARY MATERIALS

Please browse Full Text version to see the data of Supplementary Materials 1 and 2.